IOSR Journal of Engineering (IOSRJEN) www.iosrjen.org
ISSN (e): 2250-3021, ISSN (p): 2278-8719 Special Issue || September 2021 || PP 55-68
7th National Conference On Advancements in Communication, Computing and Electronics Technology-ACCET 2021

Efficient Wireless Power Transfer System at Low frequency for Biomedical Implant Application

D.B.Ahire[1], Dr.Vitthal J.Gond[2], Dr.Jayant J. Chopade[3]
[1]Research Scholar, MCOERC Nashik. Maharashtra, India, dbahire21@gmail.com [2]Professor, MET's Institute of Engineering, BKC, Nashik, Maharashtra, India, vjg.eltx@gmail.com [3]Professor, MCOERC Nashik. Maharashtra, India, jchopade@yahoo.com

Abstract— *In this paper the wireless recharging of pacemaker's battery for biomedical implant is considered. The Square PCB receiving coil for Wireless power transfer system is found suitable to achieve higher coupling coefficient between primary and secondary coil. The coil is embedded inside the biomedical implant. The coil trace (w), pitch(s), thickness (t), number of turns and outer diameter (D_{out}) are the key parameters in designing the square PCB coil for higher coupling coefficient. The experimentation in simulation environment is carried for two low frequencies as 20 kHz and 300 KHz to comply EMF safety standard limits for biomedical application. The experimental results by simulation are presented for 1KΩ load. Power transfer efficiency for 20 KHz is 69.40% and 300 KHz it is 99.67%. It is observed that the power transfer efficiency is higher for higher frequencies.*

Keywords—*Wireless power transfer, pacemaker, Coupling Coefficient, Resonant Inductive coupling, power transfer efficiency*

I. Introduction

Wireless P ower Transfer (WPT) is the technology that enables a power source to transmit electromagnetic energy to an electrical load across an air gap, without interconnecting cords. This technique is rapidly growing and is applicable to the domains, including industrial applications consumer products and biomedical implant. Biomedical implanted devices are becoming popular in health and medical applications in a wide range of areas, such as, cardiac pacemakers, retinal prosthesis, cochlear implants, defibrillator, smart orthopaedic implants, and artificial hearts etc. The traditional approach of supplying power to these devices is implantable batteries, bio-fuel cell and percutaneous links. However, any battery has limited energy storage and life span, similarly bio-fuel cell has low output power and percutaneous links are susceptible to infection and reliability problems [1]-[6][21].

The current implantable devices available in the market consist of non rechargeable large sized batteries. Biomedical implants require high energy batteries to supply power for longer duration therefore bulky size of the battery is required to supply the power to biomedical implant for longer duration. Moreover since the battery is non rechargeable, it has to be removed after its life span. This necessitates costly invasive surgery to replace the battery.

Presently there is a tremendous advancement in developing rechargeable batteries which could improve the life span of pacemaker batteries by recharging wirelessly using magnetic resonance coupling [7]-[9]. In this paper the experimentation is carried out in simulation environment to optimize the geometrical parameter of primary and secondary square PCB coil with aiming to achieve higher coupling coefficient between primary and secondary coil.

1. Principle of WPT System

Wireless power transfer system can be categorized into far field and near field WPT. The radio frequency transmission, microwave applications are the few examples of far field WPT system and Biomedical application [16] [17], whereas inductive coupling, magnetic resonance coupling and capacitive coupling based methods are categorized into near field WPT system [1]-[16][19] [20][21]. In this paper magnetic resonance coupling using SP topology is chosen for higher power transfer efficiency. The general architecture of near field WPT system for biomedical implant is as shown in Fig.1and Fig.2 shows the different topologies for magnetic resonance coupling [1].

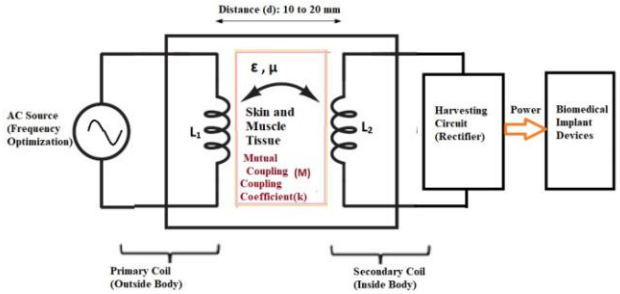

Fig.1. General Diagram of WPT for Biomedical Implant

The advantage of magnetic resonance coupling is to improve the power transfer efficiency and distance as compared to inductive coupling.

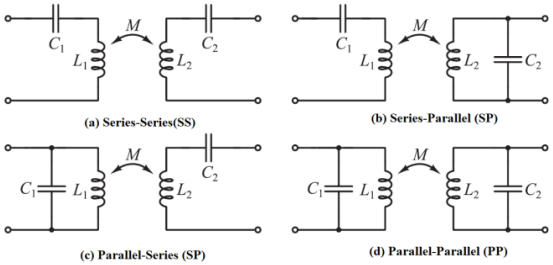

Fig.2. Different Resonant Configurations for Magnetic Resonant Coupling [1] [5].

To achieve the higher power transfer efficiency between the primary and secondary coil, the coupling coefficient between two coils should be maximum. The range of the coupling coefficient is 0 to 1.

To obtain the perfect coupling between primary and secondary coil, the flux lines must intersect the coils, this can be achieved only if both the coils are overlap. For guided path like transformer, the coupling is perfect as the coils are wound on a magnetic core having high magnetic permeability i.e. low magnetic reluctance and therefore flux line provide the guided path through the core [4].

For implant devices, the flux lines are passing through the human tissue (i.e. skin, blood, fats) having different dielectric properties at different frequency hence the coupling coefficient is less. The relation holds true for input voltage, induced secondary voltage and is govern by turn's ratio of primary and secondary coil as[4],

$$\frac{V_1}{V_2} = \frac{N_1}{N_2} \qquad (1)$$

While studying an implantable cardiac pacemaker it is observe that for different make the dimension of an implantable cardiac pacemaker is 35 x 35 mm to 40x40mm [5][6]. For simulation purpose the minimum range of the secondary coil size is considered i.e.35mm x 35mm. While taking decision of coil size and shape, the implant dimension is a constrain, hence to maximise the number of turns in a specified dimension of an implantable cardiac pacemaker, the square shape for secondary coil is finalized and to achieve maximum coupling between primary and secondary coil, the same shape of primary coil is selected. The coil design and other analysis are described in subsequent section.

II. Square PCB coil and their Inductance and Coupling Coefficient

In this section, analytical method is described to find desired electrical parameters including self inductance (L) of primary and secondary coil, mutual inductance (M) between primary and secondary coil, Coupling Coefficient (k) between primary and secondary coil.

The experimentation in simulation environment for differing geometry and size is studied. It is noted that a square shape of coil is giving better results as compare to other geometrical structures [1]. The Fig.3 shows the coil geometry selected for further investigation.

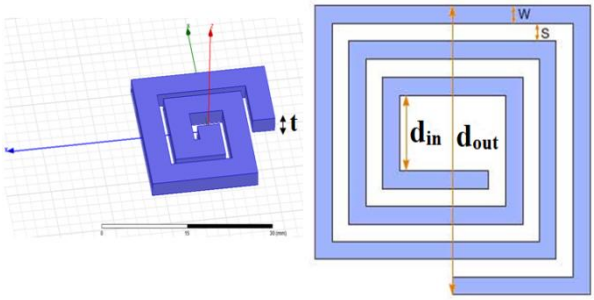

Fig.3. Geometrical parameters of square PCB coil.

As shown in Fg.3, the different geometrical parameters of square PCB coil are trace (w), pitch (s), outer diameter (d_{out}), inner diameter (d_{in}) and thickness (t). Numbers of
turns of the primary and secondary coils are governing by equation (1).

Analytic methods are well described in the literature for calculation of inductance of square PCB coil based on their geometrical parameters, Wheeler presented several formulas for planar spiral discrete inductors [1]. A simple modification of the original Wheeler formula gives an expression for Square PCB inductors,

$$L_{mw} = 2.34\mu_0 \frac{n^2 d_{avg}}{1+2.75\,\rho} \qquad (2)$$

Where ρ is the fill ratio: $\rho = (d_{out} - d_{in})/ (d_{out} + d_{in})$
$d_{avg} = 0.5\ (d_{out} + d_{in})$
μ_0= Permeability in free Space
n= Number of turns of square PCB coil
d_{out} =Outer diameter of square PCB coil
d_{in}= Inner diameter of square PCB coil

Similarly, Simple and accurate expression for the inductance of a planar spiral (square PCB coil) can be obtained by approximating the sides of the spirals by symmetrical current sheets of equivalent current densities using the concepts of Geometric Mean Distance (GMD) [1] [15].

$$L_{gmd} = \frac{1.27\mu_0 n^2 d_{avg}}{2}\left(\ln\left(\frac{1.07}{\rho}\right) + 0.18\,\rho + 0.13\rho^2\right) \qquad (3)$$

Analytical method for calculation of mutual inductance of coaxial circles using elliptic integrals is given by Maxwell [1] ,

$$M = 4\pi\sqrt{Aa}\left\{\left(\frac{2}{k} - k\right)F - \frac{2}{k}E\right\} \qquad (4)$$

Where **A** and **a** are the radii of the two circles, d is the distance between their centers, and

$$k = \frac{2\sqrt{Aa}}{\sqrt{(A+a)^2+d^2}} = \sin\gamma = \frac{\sqrt{r_1^2 - r_2^2}}{r_1} \qquad (5)$$

F and E are the complete elliptic integrals of the first and second kind, respectively, to modulus k. Their values may be obtained from the tables of Legendre.
Soma and Galbraith have discussed a practical treatment of mutual inductance calculation, where each coil is considered as a series of circular filaments, each being coupled to all other filaments, dependent on their physical arrangement and also discuss the coaxial, lateral and angular displacement in detail[1].

The coupling coefficient between to coil can be expressed using mutual inductance and self inductance of both coils as [1] [15]

$$k = \frac{M}{\sqrt{L_1 L_2}} \qquad (6)$$

The amount of inductive coupling that exists between the two coils is expressed as a fractional number between 0 and 1, if k = 1 the two coils are perfectly coupled, if k > 0.5 the two coils are said to be tightly coupled and if k < 0.5 the two coils are said to be loosely coupled.

Resistance or series loss of the coil can be categories into three parts as [1],

$$R = R_{DC} + R_{skin} + R_{prox} \quad (7)$$

Where R_{DC} is the simple resistive loss or DC resistance of the conductor, R_{skin} is the loss due to the skin effect and R_{prox} is the loss due to the proximity effect [1].

$$R_{DC} = \rho \frac{l_c}{A_c} \quad (8)$$

ρ = Resistivity of the material
l_c = Length of the conductor
A_c = Cross Sectional area of the Conductor

The skin effect is the formation of a thin 'skin' of current at the edges of a conductor that is carrying high frequency current. The proximity effect is another kind of the resistive loss that occurs due to adjacent current filament flowing in the same direction. The loss is more effective if the filaments are closer to each other at high frequency. At low frequency, the skin effect and proximity losses are negligible therefore only simple resistive losses are considered. Thus the equivalent circuit diagram of WPT system (non-perfect coupling) in terms of Electrical parameters as shown in figure 4.

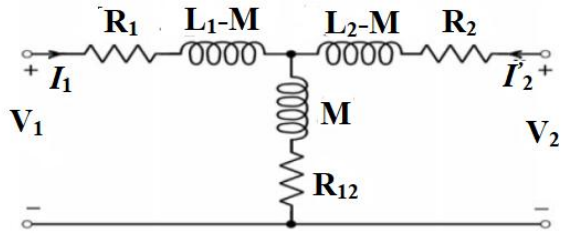

Fig.4. Equivalent circuit diagram of WPT system (non-perfect coupling) in terms of Electrical parameters

For analytical method, to calculate electrical parameters of optimized geometrical parameters, Coupled coil Configurator (CuCCo) software is used [35]. Comparative results between analytical and simulation methods are described in subsequent section.

III. Electrical Parameters of Square PCB Coil using Simulation Method

The process starts with constraint which includes size of implanted secondary coil (35mm x 35mm), the primary coil which is placed outside the body is varied from 40mm to 70mm for achieving maximum coupling coefficient, distance between primary coil and secondary coil is kept 10mm, Model is simulated at 20 KHz and 300KHz frequency.

Electrical parameters from geometrical parameters of square PCB coil are obtained using FEM Simulation. Optimetrics tool is also used for finding maximum coupling and other electrical parameters of square PCB coil from specified range of geometrical parameters. Electrical parameters are determined at two different frequencies as 20 KHz and 300 KHz using Eddy current solver. Dielectric properties of human tissue parameters (Skin, blood, fat) at 20 KHz and 300 KHz are selected [25]. Table 1 shows the geometrical and Electrical parameters of square PCB coil. Table 2 shows the coil material and substrate properties similarly Table 3 shows dielectric properties of the human tissue parameters at 20 KHz and 300 KHz [25].

Table 1: Geometrical and Electrical parameters

Geometrical Parameter	d_{out}	Outer diameter
	w	Trace
	s	Pitch
	t	Thickness
	N_1,N_2	Number of turns of Primary and Secondary Coil
Electrical Parameter	L_1,L_2	Inductance of Primary (Tx) and Secondary (Rx) coil
	M	Mutual inductance
	k	Coupling Coefficient

	R_1,R_2	Resistance of Primary (Tx) and Secondary (Rx) coil
	R_{12}	Resistance between Primary (Tx) and Secondary (Rx) coil

Table 2: Coil material and substrate properties [26] [27*]*

Primary Coil	Copper	Relative Permittivity (ε_r)	1
		Relative Permeability (μ_r)	0.99
		Conductivity(σ)	58000000 Siemens/m
Secondary Coil and Pacemaker case	Titanium	Relative Permittivity (ε_r)	1
		Relative Permeability(μ_r)	1.00018
		Conductivity (σ)	1820000 Siemens/m
Substrate below primary coil	Ferrite	Relative Permittivity (ε_r)	12
		Relative Permeability(μ_r)	1000
		Conductivity (σ)	0.01 Siemens/m
	FR4	Relative Permittivity (ε_r)	4.4
		Relative Permeability(μ_r)	1
		Conductivity(σ)	0
Substrate above Secondary coil	Polyurethane	Relative Permittivity (ε_r)	2.25
		Relative Permeability(μ_r)	1
		Conductivity(σ)	0 Siemens/m

.

Table3: Dielectric properties of human body parameters at 20 KHz and 300 KHz [25]

Tissue	Dielectric Properties		Frequency	
			20KHz	300KHz
Blood	Permittivity (ε_r)		5000	5000
	Conductivity (σ) Siemens/m		0.7	0.7
Fat	Infiltrate	Permittivity (ε_r)	400	50
		Conductivity (σ) Siemens/m	0.05	0.05
	Not Infiltrate	Permittivity (ε_r)	300	40
		Conductivity (σ) Siemens/m	0.03	0.03
Skin	Dry	Permittivity (ε_r)	1000	1000
		Conductivity(σ) Siemens/m	0.0002	0.002
	wet	Permittivity (ε_r)	30000	5000
		Conductivity(σ) Siemens/m	0.005	0.2

In this paper, the primary goal is to identify the maximum coupling by varying geometrical parameters of primary and secondary coil. Geometrical parameter such as thickness (t), pitch (s), trace (w) and outer diameter are optimized and results for different cases are as shown in Table 4 to Table 17

Case: 1 Number of Turns: N_1 =4, N_2 = 2

Table 4: Thickness (t) Optimetrics (60mm x 35mm)

Coil Dimension	Dout	Primary Coil (Tx)	60mm		
		Secondary Coil (Rx)	35mm		
Constant Parameters	Trace (w)		4mm		
	Pitch (s)		0.5mm		
Frequency	300KHz				
Thickness(t) Optimetrics					
Tx Coil (µm)	Rx Coil (µm)	K	L_1 (nH)	L_2 (nH)	M (nH)
25	25	0.094	429.94	131.50	22.57
30	30	0.095	423.39	132.03	22.42
35	35	0.11	419.49	149.01	25.03
40	40	0.093	413.38	129.83	21.65
45	45	0.093	410.19	129.30	21.53
50	50	0.092	407.10	129.13	21.28

Table 5: Pitch (s) Optimetrics (60mm x 35mm)

Coil Dimension	Dout	Primary Coil (Tx)	60mm
		Secondary Coil (Rx)	35mm
Constant Parameters	Trace (s)		4 mm
	Thickness (t)		0.35µm
Frequency	300KHz		
Pitch (w) Optimetrics			

Tx Coil (mm)	Rx Coil (mm)	K	L_1 (µH)	L_2 (nH)	M (µH)
0.1	0.1	0.09	958.63	138.9	35.17
0.5	0.5	0.11	942.6	131.7	38.9
1	1	0.08	631.4	123.8	23.08
1.5	1.5	0.09	620.5	118.3	25.50
2	2	0.05	354.9	112.1	11.76

Table 6: Trace (w) Optimetrics (60mm x 35mm)

Coil Dimension	Dout	Primary Coil (Tx)	60mm
		Secondary Coil (Rx)	35mm
Constant Parameters	Pitch (p)		0.5mm
	Thickness (t)		0.35µm
Frequency	300KHz		

Trace (w) Optimetrics

Tx Coil (mm)	Rx Coil (mm)	K	L_1 (µH)	L_2 (nH)	M (nH)
1	1	0.078	3.48	240.38	71.83
2	2	0.117	2.50	173.08	77.35
3	3	0.153	1.82	132.64	75.56
4	3	0.110	0.94	131.79	38.90

Table 7: Outer Diameter of primary coil (Dout) Optimetrics

Coil Dimension	Dout	Secondary Coil (Rx)	35mm
Constant Parameters	Trace (w)	Primary Coil (Tx)	3mm
		Secondary Coil (Rx)	3mm
	Pitch (s)		0.5mm
	Thickness (t)		0.35µm
Frequency	300KHz		

Outer Diameter(Dout) Optimetrics

Dout (mm)	K	L_1 (µH)	L_2 (nH)	M (nH)
40	0.094	0.418	130.57	21.96
45	0.105	0.496	131.22	26.98
50	0.125	0.879	132.74	42.81
55	0.154	0.949	131.92	43.99
60	0.153	1.828	132.64	75.56
65	0.132	2.108	132.60	69.89
70	0.107	2.416	132.09	60.50

Table 8: Outer Diameter of primary coil (Dout) Optimetrics

Coil Dimension	Dout	Secondary Coil (Rx)	35mm
Constant Parameters	Trace (w)	Primary Coil (Tx)	3mm
		Secondary Coil (Rx)	3mm
	Pitch (s)		0.5mm
	Thickness (t)		0.35µm
Frequency	20KHz		

Outer Diameter(Dout) Optimetrics

Dout (mm)	K	L_1 (µH)	L_2 (nH)	M (nH)
40	0.121	0.86	176.20	47.32
45	0.157	1.36	177.08	77.36
50	0.167	1.79	177.89	97.90
55	0.179	1.95	178.10	105.65
60	0.162	2.26	179.07	103.47
65	0.134	2.59	178.39	91.66
70	0.107	2.95	179.48	78.33

Case: 2 Number of Turns: N_1 =8, N_2 = 4

Table 9: Trace (w) Optimetrics (60mm x 35mm)

Coil Dimension	Dout	Primary Coil (Tx)	60mm
		Secondary Coil (Rx)	35mm
Constant	Pitch (p)		0.5mm

Parameters	Thickness (t)				0.35µm
Frequency	300KHz				
Trace (w) Optimetrics					
Tx Coil (mm)	Rx Coil (mm)	K	L_1 (µH)	L_2 (nH)	M (nH)
1	1	0.115	6.64	549.26	220.12
1	1.5	0.118	6.65	549.26	198.26
1	2	0.120	6.64	422.29	181.39
1	2.5	0.121	6.64	338.73	163.59
1.5	2.5	0.146	5.16	273.23	173.52

Table 10: Outer Diameter of primary coil (D_{out}) Optimetrics

Coil Dimension	Dout	Secondary Coil (Rx)	35mm
Constant Parameters	Trace (w)	Primary Coil (Tx)	1.5mm
		Secondary Coil (Rx)	2.5mm
	Pitch (s)		0.5mm
	Thickness (t)		0.35µm
Frequency	300KHz		
Outer Diameter(Dout) Optimetrics			
Dout (mm)	K	L_1 (µH)	L_2 (nH)	M (nH)
40	0.110	2.317	267.65	86.81
45	0.145	3.015	269.52	131.33
50	0.165	3.725	269.94	165.82
55	0.174	4.439	269.81	180.25
60	0.146	5.169	269.60	173.52

Table 11: Outer Diameter of primary coil (D_{out}) Optimetrics

Coil Dimension	Dout	Secondary Coil (Rx)	35mm
Constant Parameters	Trace (w)	Primary Coil (Tx)	1.5mm
		Secondary Coil (Rx)	2.5mm
	Pitch (s)		0.5mm
	Thickness (t)		0.35µm
Frequency	20KHz		
Outer Diameter(Dout) Optimetrics			
Dout (mm)	K	L_1 (µH)	L_2 (nH)	M (nH)
45	0.205	1.83	333.04	160.88
50	0.200	2.30	335.46	167.31
55	0.217	3.01	336.15	189.23
60	0.208	3.31	331.76	218.93
65	0.192	3.97	339.62	223.59
70	0.167	4.66	338.39	210.94

Case: 3 Number of Turns: N_1 =12, N_2 = 8

Table 12: Trace (w) Optimetrics (60mm x 35mm)

Coil Dimension	Dout	Primary Coil (Tx)	60mm
		Secondary Coil (Rx)	35mm
Constant Parameters	Pitch (p)		0.5mm
	Thickness (t)		0.35µm
Frequency	300KHz		
Trace (w) Optimetrics			
Tx Coil (mm)	Rx Coil (mm)	K	L_1 (µH)	L_2 (µH)	M (µH)
1	1	0.154	10.27	0.822	0.449
1	1.5	0.156	10.28	0.587	0.383
1.1	1.6	0.162	9.55	0.551	0.372
1.2	1.7	0.166	8.83	0.511	0.353

Table 13: Outer Diameter of primary coil (D_{out}) Optimetrics

Coil Dimension	Dout	Secondary Coil (Rx)	35mm
Constant Parameters	Trace (w)	Primary Coil (Tx)	1.2mm
		Secondary Coil (Rx)	1.7mm
	Pitch (s)		0.5mm

	Thickness (t)			0.35µm
Frequency	300KHz			
Outer Diameter(Dout) Optimetrics				
Dout (mm)	K	L_1 (µH)	L_2 (nH)	M (nH)
40	0.104	4.916	582.06	171.98
45	0.142	5.695	580.02	259.77
50	0.165	7.208	584.89	340.62
55	0.177	8.729	586.42	383.31
60	0.156	10.283	587.15	383.74

Table 14:Outer Diameter of primary coil (D_{out}) Optimetrics

Coil Dimension	Dout	Secondary Coil (Rx)	35mm
Constant Parameters	Trace (w)	Primary Coil (Tx)	1mm
		Secondary Coil (Rx)	1.5mm
	Pitch (s)		0.5mm
	Thickness (t)		0.35µm
Frequency	20KHz		
Outer Diameter(Dout) Optimetrics			
Dout (mm)	K	L_1 (µH)	L_2 (µH)	M (µH)
40	0.112	5.04	0.71	0.22
45	0.157	5.86	0.72	0.34
50	0.189	7.42	1.004	0.51
55	0.203	9.01	1.005	0.58
60	0.182	10.64	1.007	0.59
65	0.170	13.19	1.008	0.52
70	0.128	14.18	1.009	0.48

Case: 4 Number of Turns: N_1 =16, N_2 = 8

Table 15: Trace (w) Optimetrics (60mm x 35mm)

Coil Dimension	Dout	Primary Coil (Tx)		60mm
		Secondary Coil (Rx)		35mm
Constant Parameters	Pitch (p)			0.5mm
	Thickness (t)			0.35µm
Frequency	300KHz			
Trace (w) Optimetrics				
Tx Coil (mm)	Rx Coil (mm)	K	L_1 (µH)	L_2 (µH)	M (nH)
1	1	0.1658	16.72	1.302	774.07
1.2	1.2	0.1762	13.636	1.080	676.30
1.2	1.4	0.1763	13.639	0.905	619.88
1.2	1.5	0.1761	13.646	0.831	593.35

Table 16: Outer Diameter of primary coil (D_{out}) Optimetrics

Coil Dimension	Dout	Secondary Coil (Rx)	35mm
Constant Parameters	Trace (w)	Primary Coil (Tx)	1.2mm
		Secondary Coil (Rx)	1.4mm
	Pitch (s)		0.5mm
	Thickness (t)		0.35µm
Frequency	300KHz		
Outer Diameter(Dout) Optimetrics			
Dout (mm)	K	L_1 (µH)	L_2 (µH)	M (nH)
40	0.102	7.60	1.284	320.84
45	0.143	8.92	1.287	485.85
50	0.168	11.47	1.299	651.17
55	0.180	15.33	1.297	737.00
60	0.166	16.73	1.305	777.29

Table 17: Outer Diameter of primary coil (D_{out}) Optimetrics

Coil Dimension	Dout	Secondary Coil (Rx)	35mm
Constant Parameters	Trace (w)	Primary Coil (Tx)	1.2mm
		Secondary Coil (Rx)	1.2mm

	Pitch (s)			0.5mm
	Thickness (t)			0.35µm
Frequency	20KHz			
Outer Diameter(Dout) Optimetrics				
Dout (mm)	K	L_1 (µH)	L_2 (µH)	M (nH)
40	0.121	7.81	1.594	0.429
45	0.167	9.17	1.591	0.640
50	0.195	11.79	1.590	0.848
55	0.204	14.50	1.595	0.983
60	0.192	17.22	1.576	1.003
65	0.169	20.19	1.598	0.963
70	0.154	21.63	1.595	0.909

Following table show the Summarize report of different cases

Table: 18 Summary reports of different cases

Number of Turns		Geometrical Parameters					Coupling (k)	
Tx	Rx	t	s	Trace (w)		D_{out} of Tx Coil (mm)	20 KHz	300 KHz
		Tx and Rx (µm)	Tx and Rx (mm)	Tx (mm)	Rx (mm)			
4	2	35	0.5	3	3	55	0.18	0.15
8	4	35	0.5	1.5	2.5	55	0.21	0.17
12	6	35	0.5	1.2	1.7	55	0.20	0.18
16	8	35	0.5	1.2	1.4	55	0.20	0.18

From the comparative study of summary report, it is found that, the case-2 is more promising as it gives maximum coupling coefficient. 3D Model for case-2 is shown in Fig. 5

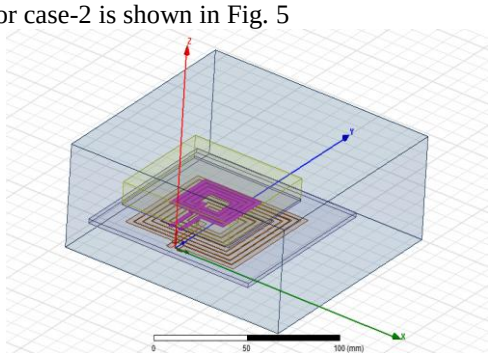

Fig.5: 3D Model of square PCB coil in Ansys Maxwell.

Electrical parameters as shown in figure 4 for selected geometry are extracted using Maxwell Simulation tool and extracted Electrical parameters at 20KHz and 300Khz are shown in Table 20 below,

Table: 20 Extracted Electrical Parameters at 20 KHz and 300 KHz.

Electrical parameters	Eddy Current Solver	
	20 KHz	300 KHz
Primary Inductance (L_1)	4.62	4.43
Secondary Inductance (L_2) (µH)	0.336	0.269
Mutual Inductance (M) (µH)	0.241	0.180
Primary Resistance(R_1)	0.448	0.592
Secondary Resistance (R_2) (Ω)	2.74	2.76
Mutual Resistance (R_{12})	0.008	0.033
Coupling Coefficient (k)	0.21	0.17

IV. Magnetic Resonance Coupling and Power transfer efficiency using Simplorer

Simplorer circuit simulation tool is used for finding the power transfer efficiency of Magnetic Resonance WPT. Among the four possible combinations of the two resonant circuits as shown in Fig. 2, for biomedical implant application, SP topology is best suited for magnetic resonance WPT [1], since for high power transfer efficiency, input impedance should be low while output impedance should be high. In the case SP topology, the tuned capacitances C1 and C2, at resonant frequency,$\omega_r = 2\pi f_r$ are [2] [28];

$$C_1 = \frac{1}{\omega_r^2(1-k^2)L_1} \quad (9)$$

$$C_2 = \frac{1}{\omega_r^2 L_2} \quad (10)$$

The values for C_1 and C_2 are obtained for selected geometry from table 20 at 20 KHz and 300 KHz frequency. Power Transfer Efficiency (PTE) using Simplorer circuit simulation tool at load 10Ω,100Ω,1KΩ and 10KΩ keeping source resistance Rs=1Ω constant are obtained as shown in fig.6 to fig.13 below,

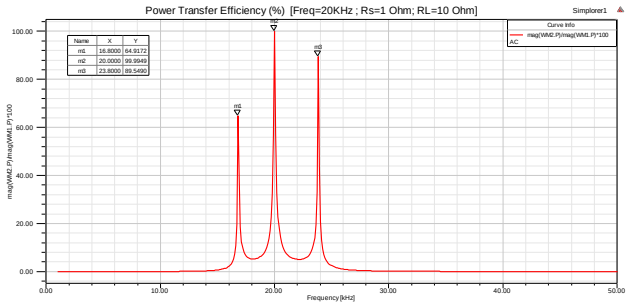

Fig.6 Power Transfer Efficiency (%) at 20 KHz (R_L=10Ω)

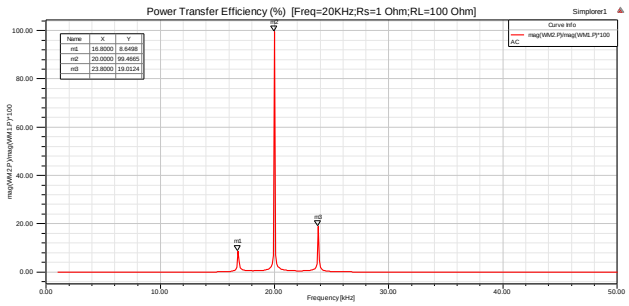

Fig.7 Power Transfer Efficiency (%) at 20 KHz (R_L=100Ω)

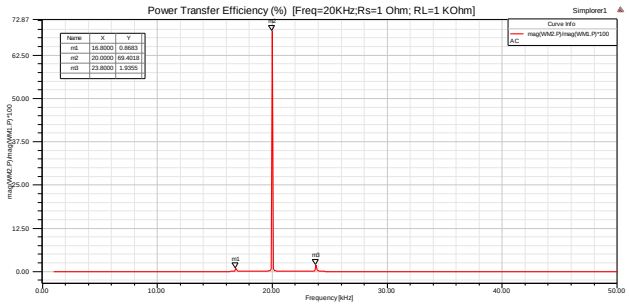

Fig.8 Power Transfer Efficiency (%) at 20 KHz (R_L=1kΩ)

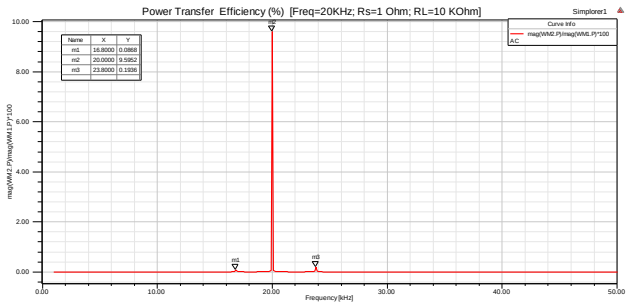

Fig.9 Power Transfer Efficiency (%) at 20 KHz (R_L=10kΩ)

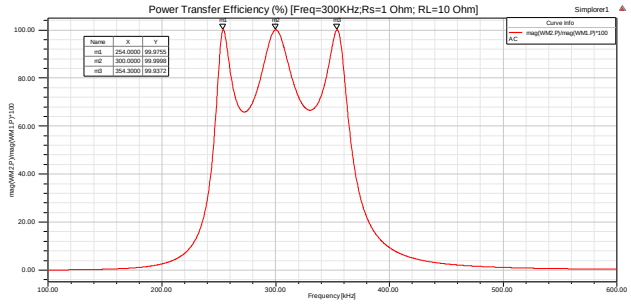

Fig10 Power Transfer Efficiency (%) at 300 KHz (R_L=10Ω)

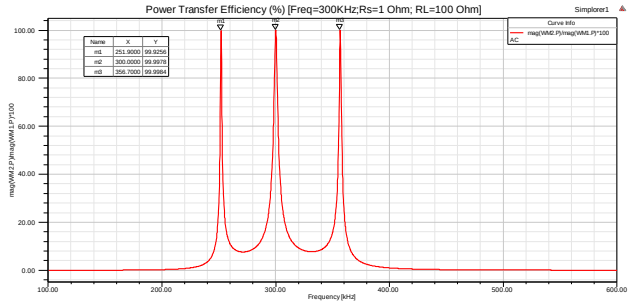

Fig11 Power Transfer Efficiency (%) at 300 KHz (R_L=100Ω)

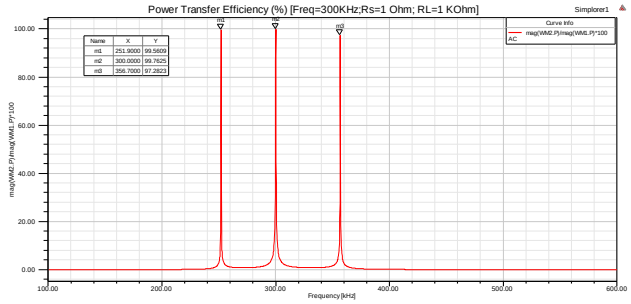

Fig12 Power Transfer Efficiency (%) at 300 KHz (R_L=1KΩ)

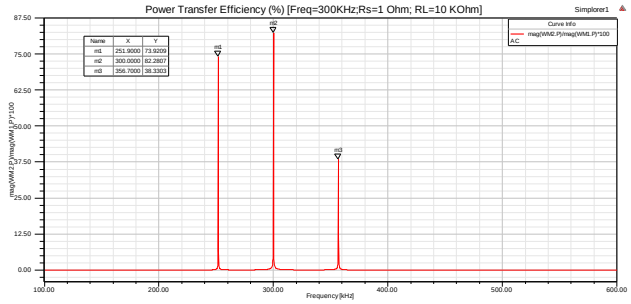

Fig13 Power Transfer Efficiency (%) at 300 KHz (R_L=10kΩ)

Summary of power transfer efficiency at 20 KHz and 300 KHz at different load is shown in Table 21 below,

Table 21: Power Transfer Efficiency (PTE) at 20 KHz and 300 KHz for different load

Load Resistance (R_L)Ω	Power Transfer Efficiency (PTE) (%)	
	20 KHz	300 KHz
10Ω	99.99	99.99
100Ω	99.46	99.99
1kΩ	69.40	99.67
10kΩ	9.59	82.28

The comparison of electrical parameters obtained by simulation and analytical method are shown in Table 22.

Table 22: Comparison of Magnetic Resonance WPT using Simulation and Analytical method

Parameters	Simulation Method		Analytical Method	
	20KHz	300KHz	20KHz	300KHz
Primary coil Inductance (L_1)(µH)	4.62	4.43	4.08	4.08
Secondary coil Inductance (L_2) (µH)	0.336	0.269	0.588	0.558
Mutual Inductance (M) (µH) at 10mm distance	0.241	0.180	0.11	0.11
Coupling Coefficient (k) at 10mm distance	0.21	0.17	0.13	0.11
Primary coil Resistance(R_1)	0.448	0.592	0.447	0.525
Secondary coil Resistance (R_2) (Ω)	2.74	2.76	2.42	2.49

V. Result and Discussion

The primary goal of wireless power transfer system is to provide sufficient power with higher efficiency to charge rechargeable battery of biomedical implant. To achive higher power transfer efficiency, the coupling coefficient between primary and secondary coil should be high. So in this paper, geometrical parameters are selected using optimetric tool for achiving higher coupling at selected frequency. The elecrical parameters are extracted for same frequency using simulation method. Analytical method is used to compare the electrical parameters of selected geometry. It is observed that results obtained using simulation method are in close agreement with result obtained using approximate analytical method. In the proposed model, for primary (TX) coil, copper material is used for coil and FR4 ferrite dielectric is used as a substrate (shield) and for biomedical implant application, biocompatible titanium material is used for secondary square PCB coil and polyurethane dielectric is used as a substrate. Biological tissues are considered as a medium between primary and secondary coil. At lower frequencies, biological tissue can be considered to have $\mu = \mu_0$ and ε is more variable and dependent on tissue type [25]. Analytic calculations become more complex for environments containing layers of material with different permittivity's [1] therefore in this paper, for accurate measurement of electrical parameters and PTE from selected geometry, FEM based simulations is used. To improve the WPT performance not only coupling coefficient is important but quality factor (Q) of both the coils also be considered but Q factor is higher with frequency therefore it is necessary to consider higher frequencies to improve the WPT performance. To prevent the frequency splitting phenomenon, the optimum selection of distance between to the coils and mutual inductance is necessary in future. Physical measurements using experimental method is necessary to validate these performance parameters may be necessary in future.

VI. Conclusions

Simulation method is used to perform the experimentation to achieve higher coupling coefficient form geometrical parameters of primary and secondary square PCB coil using Optimetrics tool, and electrical parameters extracted by simulation method are compared with analytical method and found very close approximation. Higher PTE of optimized geometrical parameters is found using Magnetic Resonance, Experimentation is done using Circuit simulation tool. WPT.SP topology is used for Magnetics resonance and it is found that power transfer efficiency decreased as is load increased. Also it is noted that power transfer efficiency increases for higher source frequency, but to comply EMF safety standard limits for biomedical application lower source frequency is selected. Power transfer efficiency at 1KΩ for 20 KHz and 300 KHz is 69.40% and 99.67% achieved respectively. Frequency splitting in WPT system is caused by the magnetic over-coupling between the transmitter and the receiver coil. The key point of the frequency splitting elimination is maintaining the value of k much less than 1 for any distance to avoid the pole while determining the value of mutual inductance similarly physical measurements using experimental method is necessary to validate PTE for selected geometry and frequency may be necessary in future.

Acknowledgment

I am very thankful to MET's, Institute of Engineering, Bhujbal Knowledge City, Nashik, Matoshri College of Engineering and Research Canter, Nashik and K. K. W. Institute of Engineering Education and Research, Nashik for providing me resources required for my research work.

References

[1]. M. Schormans, V. Valente, and A. Demosthenous, "Practical Inductive Link Design for Biomedical Wireless Power Transfer: A Tutorial," IEEE Transactions on Biomedical Circuits and System, Vol. 12, no.5, pp.1112-1130, Oct. 2018

[2]. C. Liu, C. Jiang, J. Song and K. T. Chau, "An Effective Sandwiched Wireless Power Transfer System for Charging Implantable Cardiac Pacemaker," in *IEEE Transactions on Industrial Electronics*, vol. 66, no. 5, pp. 4108-4117, May 2019.

[3]. S. A. Mirbozorgi, P. Yeon, M. Ghovanloo ,"Robust Wireless Power Transmission to mm-Sized Free-Floating Distributed Implants," IEEE Transactions on Biomedical Circuits and Systems ,Vol. 11, no. 3,pp.692-702, June 2017

[4]. V. Vulfin, S. Sayfan-Altman and R. Ianconescu, "Wireless power transfer for a pacemaker application," Journal of Medical Engineering & Technology, 41(4):1-8, Taylor and Francis Group, March 2017

[5]. T.Campi, S. Cruciani, F. Palandrani, V. De Santis, A. Hirata, M. Feliziani, " Wireless Power Transfer Charging System for AIMDs and Pacemakers," IEEE Transactions on Microwave Theory and Techniques, Vol. 64, no. 2,pp.633-642, Feb. 2016.

[6]. T. Campi, S. Cruciani, V. De Santis, and M. Feliziani, "EMF Safety and Thermal Aspects in a Pacemaker Equipped With a Wireless Power Transfer System Working at Low Frequency," IEEE Transactions on Microwave Theory and Techniques, Vol. 64, no. 2, pp.375-382, Feb.2016.

[7]. D. Jiang, D. Cirmirakis, M. Schormans, T. A. Perkins, N. Donaldson and A. Demosthenous, "An Integrated Passive Phase-Shift Keying Modulator for Biomedical Implants With Power Telemetry Over a Single Inductive Link," IEEE Transactions on Biomedical Circuits and Systems, Vol.11, no. 1,pp. 64-77, Feb. 2017.

[8]. G. Monti, P. Arcuti, L. Tarricone, "Resonant Inductive Link for Remote Powering of Pacemakers," IEEE Transactions on Microwave Theory and Techniques, Vol. 63, no. 11, pp.3814-3822, Nov. 2015.

[9]. J. Nadakuduti, M. Douglas, Lin Lu, A. Christ, P. Guckian and N. Kuster, "Compliance Testing Methodology for Wireless Power Transfer Systems," IEEE Transactions on Power Electronics, vol. 30, no. 11, pp.6264-6273 Nov. 2015..

[10]. Rui-Feng Xue, Kuang-Wei Cheng and Minkyu Je, "High-Efficiency Wireless Power Transfer for Biomedical Implants by Optimal Resonant Load Transformation," IEEE Transactions on Circuits and Systems I: Regular Papers , vol. 60, no.4 , pp.867-874, April 2013.

[11]. Meysam Zargham,P. Glenn Gulak, "Maximum Achievable Efficiency in Near-Field Coupled Power-Transfer Systems," IEEE Transactions on Biomedical Circuits and Systems , vol. 6, no. 3, pp.228-245, June 2012.

[12]. Anil Kumar RamRakhyani, Shahriar Mirabbasi and Mu Chiao, "Design and Optimization of Resonance-Based Efficient Wireless Power Delivery Systems for Biomedical Implants," IEEE Transactions on Biomedical Circuits and Systems,vol. 5,no. 1, pp.48-63, Feb. 2011.

[13]. M. Kiani and M. Ghovanloo, "An RFID-Based Closed-Loop Wireless Power Transmission System for Biomedical Applications," IEEE Transactions on Circuits and Systems II: Express Briefs, vol. 57, no. 4, pp.260-264, April 2010

[14]. Uei-Ming Jow and M. Ghovanloo, "Modeling and Optimization of Printed Spiral Coils in Air, Saline, and Muscle Tissue Environments," IEEE Transactions on Biomedical Circuits and Systems, vol. 3, no. 5, pp.339-347, Oct. 2009.

[15]. Ahire Dnyaneshwar and Kharate Gajanan, "Notch to Radiating Edge with Novel Loading of Capacitance to Wideband Microstrip Patch Antenna," International Journal of Scientific & Technology Research, vol. 9, no.01, Jan. 2020.

[16]. D.D.Ahire and G.K. Kharate, "Dual Band Microstrip Patch Antenna for Wireless Applications," International Journal of Control Theory and Applications, vol.10, no.8, pp. 167-175, 2017

[17]. Mohamad Abou Houran,Xu Yang and Wenjie Chen, "Magnetically Coupled Resonance WPT: Review of Compensation Topologies, Resonator Structures with Misalignment, and EMI Diagnostics,"MPDI, vol.7.no.11, 296,*Electronics* 2018

[18]. L. KahMeng, L. K. Yun, T. TianSwee, Ahmad Z. Md. Khudzari and S. B. Kadiman, "Wireless Power Transfer System for Biomedical Devices by using Magnetic Resonance Coupling Technique," Research Journal of Applied Sciences, Engineering and Technology, 12(8), pp.823-827, April 2016

[19]. S. Mehri, A. C. Ammari, J. B. Hadj Slama and Hatem Rmili, "Geometry Optimization Approaches of Inductively Coupled Printed Spiral Coils for Remote Powering of Implantable Biomedical Sensors," Journal of Sensors. Volume 2016, Article ID 4869571, March 2016.

[20]. Hasgall PA, Di Gennaro F, Baumgartner C, Neufeld E, Lloyd B, Gosselin MC, Payne D, Klingenböck A, Kuster N, "IT'IS Database for thermal and electromagnetic parameters of biological tissues," Version 4.0, May 15, 2018.

[21]. James B. Jarvis, M.D. Janezic, B.F.Johnk, P. Kabos, C.L. Holloway, R.G. Geyer and C.A. Grosvenor, "Measuring the Permittivity and Permeability of Loss Materials :Solids,Liquids,Metals,Building Materials and Negative-Index Materials," Electromagnetics Division, National Institute of Standards and Technology, Boulder, Co 80305,Feb.2005

[22]. Engineering ToolBox, (2010). *Relative Permittivity - the Dielectric Constant*. [online] Available at: https://www.engineeringtoolbox.com/relative-permittivity-d_1660.html.

[23]. S. Cruciani,T. Campi, F. Maradei and M. Feliziani, "Numerical simulation of Wireless Power Transfer system to recharge the battery of an implanted cardiac pacemaker," IEEE International Symposium on Electromagnetic Compatibility, pp.44-47,Gothenburg,Sweden Sept.2014.

[24]. Ashraf B. Islam, Syed K. Islam and Fahmida S. Tulip, "Design and Optimization of Printed Circuit Board Inductors for Wireless Power Transfer System," Circuits and Systems,vol.04,no.02,pp.237-244,April 2013

[25]. A. Khripkov, W. Hong and K. Pavlov, "Integrated Resonant Structure for Simultaneous Wireless Power Transfer and Data Telemetry," IEEE *Antennas and Wireless Propagation Letters*, vol. 11, pp. 1659-1662, Dec.2012.

[26]. S. Kim, J. Ho, L. Y. Chen and Ada S.Y.Poon, "Wireless power transfer to a cardiac implant," Applied Physics Letters, American Institute of Physics, 101, 073701, Aug.2012.

[27]. K. Jung, Y. Kim, E. J. Choi, H. J. Kim and Y. Kim, "Wireless power transmission for implantable devices using inductive component of closed-magnetic circuit structure," *IEEE International Conference on Multisensor Fusion and Integration for Intelligent Systems*, Seoul, pp. 272-277, Aug.2008.

[28]. "GNU general public license," Free Software Foundation. 2007. [Online] Available: http://www.gnu.org/licenses/gpl.html.

Dnyaneshwar B Ahire, M.E. (Electronics) from Govt.College of Engineering, Dr.B.A.M.University Aurangabad. The area of interest is Wireless Power Transfer system, Electromagnetics and signal Processing.

Presently working as a Assistant Professor at MET's Institute of Engineering, Bhujbal Knowledge City, Nashik in the department of Electronics and Telecommunication Engineering.

Dr. Vitthal J. Gond has completed his Ph. D. in Electronics and Communication from M. A. National Institute of technology and M.Tech in Electronics Design Technology from CEDTI. His area of interest is Optoelectronics, Integrated Power System and microelectronics. Presently he is working as a Professor, MET's Institute of Engineering, Bhujbal Knowledge City, Nashik.

Dr. Jayant J Chopade has completed his Ph.D. in Electronics and Telecommunication from savitribai Phule Pune university and M.Tech in Electronics from Visvesvaraya National Institute of Technology (VNIT Nagpur), formerly Visvesvaraya Regional College of Engineering, Nagpur (VRCE).

His area of interest is speech processing, Power electronics. Presently he is working as a Professor, MCOERC, Nashik.